

Order-disorder in the Jahn-Teller transition of LaMnO_3 : A Raman scattering study

E. Granado,* J. A. Sanjurjo, and C. Rettori

Instituto de Física "Gleb Wataghin," UNICAMP, 13083-970, Campinas-SP, Brazil

J. J. Neumeier

Department of Physics, Florida Atlantic University, Boca Raton, Florida 33431

S. B. Oseroff

San Diego State University, San Diego, California 92182

(Received 9 December 1999)

The high- T "orthorhombic-cubic" Jahn-Teller (JT) transition of a polycrystalline sample of LaMnO_3 is studied by Raman scattering. A CaMnO_3 ceramic sample is used as a reference compound. Dramatic broadening of the LaMnO_3 Raman modes are observed as T approaches the JT transition temperature (T_{JT}) from below. The strong T dependence of the phonon linewidth suggests that considerable lattice disorder is already present at temperatures well below T_{JT} . Our results indicate that the JT transition in LaMnO_3 is of order-disorder type and is driven by thermally activated e_g orbital disorder of the Mn^{3+} ion in the MnO_6 octahedra.

Manganese perovskites with the general formula $R_{1-x}A_x\text{MnO}_3$ (R =rare earth, A =Ca, Sr, or Ba) have attracted much attention, due to the discovery of a colossal magnetoresistance (CMR) effect in some of these compounds.¹ In addition to the early double exchange (DE) model,² a large electron-phonon interaction, enhanced by the strong Jahn-Teller (JT) character of Mn^{3+} ions, has been invoked to explain the magnitude of the resistivity drop and the CMR effect of doped compounds near the ferromagnetic-paramagnetic (FM-PM) transition temperature (T_C).³ The most evident manifestation of the JT effect in manganese perovskites is in the parent orthorhombic compound LaMnO_3 , which is an A -type antiferromagnetic (A -AFM) insulator.⁴ In this material only the Mn^{3+} ions are present, and a cooperative JT distortion of the MnO_6 octahedra develops due to the ordering of the $\text{Mn}^{3+} e_g$ orbitals.⁵ This orbital ordering produces a large difference between the \mathbf{a} , $\mathbf{b}/\sqrt{2}$, and \mathbf{c} orthorhombic ($Pnma$ space group) lattice parameters.⁶⁻¹³ Considerable effort has been devoted to understand the physical properties of this compound. Most of the theoretical and experimental work in LaMnO_3 concerns the correlations between magnetic and structural properties at low T .^{4,5,12-14} However, the influence of the JT distortion on the stabilization of the A -AFM alignment is still a subject of discussion.¹⁴ Another interesting point in the study of this material is the JT transition itself that occurs at high T . For nearly stoichiometric samples, the average crystal structure changes from strong orthorhombically distorted to nearly cubic above $T_{JT} \sim 700-750$ K.⁷⁻⁹ Also, dramatic changes in the magnetic correlations^{8,15,16} and in the conductivity¹⁵ were observed at T_{JT} . Millis pointed out,¹⁷ by fitting a mean-field theory to structural data in LaMnO_3 , that the basic JT energy is much larger than the stiffness parameter which orients the distortions from site to site. Based on these calculations, it was predicted that the orthorhombic-cubic transition at T_{JT} is of an order-disorder type (see below).¹⁷ The same prediction was made by Zhao and Goodenough,¹⁵ based on the fact that

the Mn-O average distance changes little through the transition.⁹ In spite of the present interest on the effects of JT distortions in manganese perovskites, the only structural information available at the moment, obtained from diffraction experiments, is about the change of the average crystal structure across the JT transition in LaMnO_3 .⁷⁻¹⁰ Therefore further experiments are clearly necessary to clarify its character and to find out the driving mechanisms of this transition.

In the last four decades, Raman spectroscopy proved to be a useful tool for the study of structural phase transitions.¹⁸ Materials presenting perovskite crystal structure, with a large number of structural changes, have been extensively studied by this technique. The phase transitions are in general classified as (i) displacive phase transitions, with the presence of at least one soft phonon with $\omega_{ph} \rightarrow 0$ as the transition temperature is approached,¹⁹ and (ii) order-disorder transitions, with a broadening of the phonon peaks, associated to the lattice disorder and the presence of a central mode near and above the transition temperature.¹⁸

In this work, Raman-scattering studies of the JT transition in LaMnO_3 are presented. A scenario for the JT transition in LaMnO_3 , consistent with our experimental results, is suggested.

The LaMnO_3 sample studied in this work was prepared by standard ceramic methods: heating stoichiometric mixtures of the corresponding oxides,²⁰ heat treatment in Ar at 900 °C for 48 h, and cooling at 100 °C/h. The structure and phase purity of the sample were checked by x-ray powder diffraction. The room-temperature lattice parameters ($Pnma$) of our LaMnO_3 sample are $\mathbf{a}=5.724(1)$ Å, $\mathbf{b}=7.696(1)$ Å, and $\mathbf{c}=5.534(1)$ Å, and are consistent to those expected for nearly stoichiometric LaMnO_3 .⁷ The spacial homogeneity of the sample was checked by previous Raman-scattering measurements.¹³ The preparation of the CaMnO_3 reference sample is described elsewhere.²¹ Magnetization measurements were taken in a vacuum of 10^{-3} torr

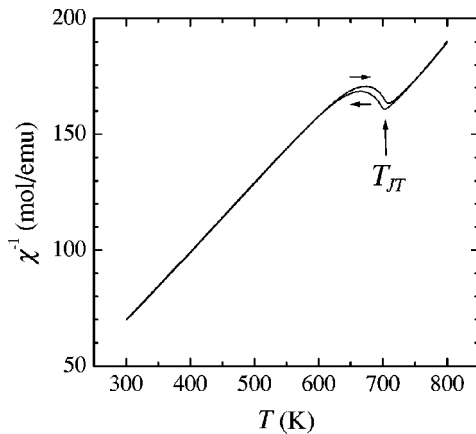


FIG. 1. T dependence of the inverse susceptibility of LaMnO_3 taken at an applied field of 1 T.

in a Quantum Design superconducting quantum interference device (SQUID) magnetometer. Raman measurements were performed in a pseudobackscattering geometry using a Jobin Yvon T64000 triple spectrometer (instrumental linewidth: $\sim 3 \text{ cm}^{-1}$) equipped with a cryogenic charge-coupled device camera, using the 514.5-nm line of an argon ion laser. The laser power was kept below 1 kW/cm^2 . Previous measurements indicate that under these conditions sample heating effects are not important for undoped LaMnO_3 .^{13,22} For the high- T Raman measurements, fresh-broken pieces of ceramic platelets were mounted in a homemade oven under Ar flux. All the measurements as a function of T were carried out increasing T . We should mention that surface decomposition induced by laser heating in an orthorhombic LaMnO_3 sample was reported in micro-Raman measurements.²² Nevertheless, in the studied T range, all our observations were reversible, indicating that thermal-induced surface decomposition is not critical for $T \lesssim 720 \text{ K}$.

Figure 1 shows the inverse dc susceptibility of our LaMnO_3 sample between 300 and 800 K, taken upon cooling and warming the sample. A first-order-like transition is clearly observed between 640 and 710 K. The abrupt change observed in the susceptibility in this T interval is a clear manifestation of the structural Jahn-Teller transition.^{8,15} The JT transition temperature of the studied sample is $T_{JT} = 708 \text{ K}$ (warming) or $T_{JT} = 703 \text{ K}$ (cooling), consistent with data already published for nearly stoichiometric LaMnO_3 powder ceramic samples.^{7,8} However, we should mention that this value is smaller than the one observed in LaMnO_3 single crystals ($T_{JT} = 750 \text{ K}$).^{15,9} Actually, the transition temperature of our sample is similar to that of a $\text{La}_{0.975}\text{Ca}_{0.025}\text{MnO}_3$ single crystal,¹⁵ suggesting that our sample presents a $\text{Mn}^{4+}/\text{Mn}^{3+}$ ratio of $\sim 2.5\%$, which is possibly due to the presence of a small amount of Mn and La vacancies. A Curie-Weiss law fitting of the data in Fig. 1 gives $\mu_{eff} = 5.20(3) \mu_B/\text{Mn}$ for $T \leq T_{JT}$, and $\Theta_p = 64(5) \text{ K}$ for $T < T_{JT}$ and $\Theta_p = 206(10) \text{ K}$ for $T > T_{JT}$.

Raman scattering profiles of LaMnO_3 , taken at $T = 10, 290, 520,$ and 720 K are shown in Fig. 2(a). At $T = 10 \text{ K}$, all the modes are quite sharp [$\Gamma(T = 10 \text{ K}) \lesssim 10 \text{ cm}^{-1}$], indicating that our sample shows good crystalline quality at low T . According to lattice dynamic calculations, the most intense modes, at $\sim 290, \sim 490,$ and $\sim 610 \text{ cm}^{-1}$, are associated

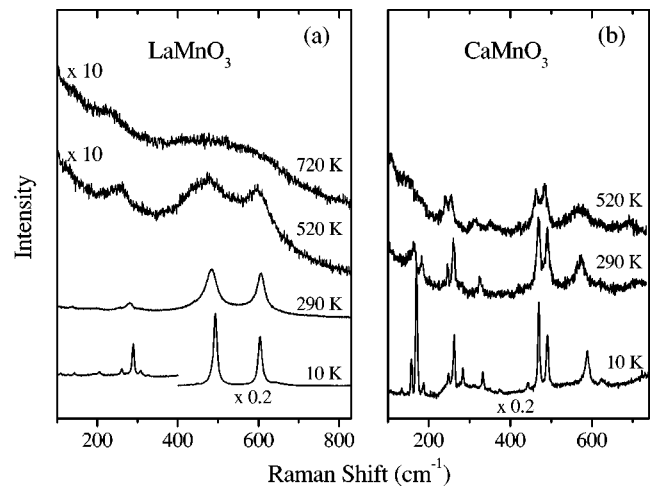


FIG. 2. Raman spectra of LaMnO_3 (a) and CaMnO_3 (b) at various temperatures. All the spectra were arbitrarily translated in the vertical.

with rotational-, bending-, and stretchinglike vibrations of the MnO_6 octahedra, respectively.²² As T increases, a dramatic broadening and intensity decrease of all the Raman modes is observed. Notice, however, that contributions from these three modes can still be identified at $T > T_{JT}$ [see Fig. 2(a) at 720 K]. For $T > 720 \text{ K}$, no relevant changes are observed in the Raman spectra of LaMnO_3 . However, at T well above T_{JT} (typically $T \approx 900 \text{ K}$), different spectra were observed for the laser focused in different regions of the sample. Strong features at $\sim 150, \sim 190,$ and $\sim 210 \text{ cm}^{-1}$ (not shown) were observed.

Figures 3(a)–(c) show, for $T < T_{JT}$, the T dependence of the linewidth for the $\sim 610-, \sim 490-,$ and $\sim 290\text{-cm}^{-1}$ peaks of LaMnO_3 , respectively (closed circles). The linewidth for the ~ 490 and $\sim 610 \text{ cm}^{-1}$ modes could not be measured above 520 K , due to the large overlapping of both peaks. For comparison, Raman measurements were also taken in ceramic samples of CaMnO_3 [see Fig. 2(b)]. This compound presents the same orthorhombic $Pnma$ perovskite crystal structure of LaMnO_3 , but only Mn^{4+} ions are present. Thus a Jahn-Teller distortion of oxygen octahedra is not expected to be present in this compound. The T dependence of the linewidths for stretching-, bending-, and rotational-like vibrations of the oxygen cage for CaMnO_3 is given in Figs. 3(a), (b), and (c), respectively (open circles). The dashed lines are the expected T dependence of the phonon linewidths according to a cubic anharmonicity in second order, i.e., $\Gamma(T) = \Gamma_0 \{1 + 2/[\exp(\hbar\omega_0/2k_B T) - 1]\}$,²³ with $\Gamma_0, \omega_0 = \Gamma_0, \omega_0(\text{CaMnO}_3)$. Although the $470-$ and 585-cm^{-1} peaks in CaMnO_3 are not exactly the same collective vibrations measured at 490 and 610 cm^{-1} in LaMnO_3 , the peak at 290 cm^{-1} in LaMnO_3 and 260 cm^{-1} in CaMnO_3 correspond to the same lattice mode, as is evident from the evolution of this mode with composition in the $\text{La}_{1-x}\text{Ca}_x\text{MnO}_3$ system.²⁴ The phonon linewidths for CaMnO_3 at low T are the same as those for the corresponding modes in LaMnO_3 (except for the bendinglike modes). However, the thermal broadenings for all observed modes are much more pronounced for LaMnO_3 . Notice that the broadening is particularly large for

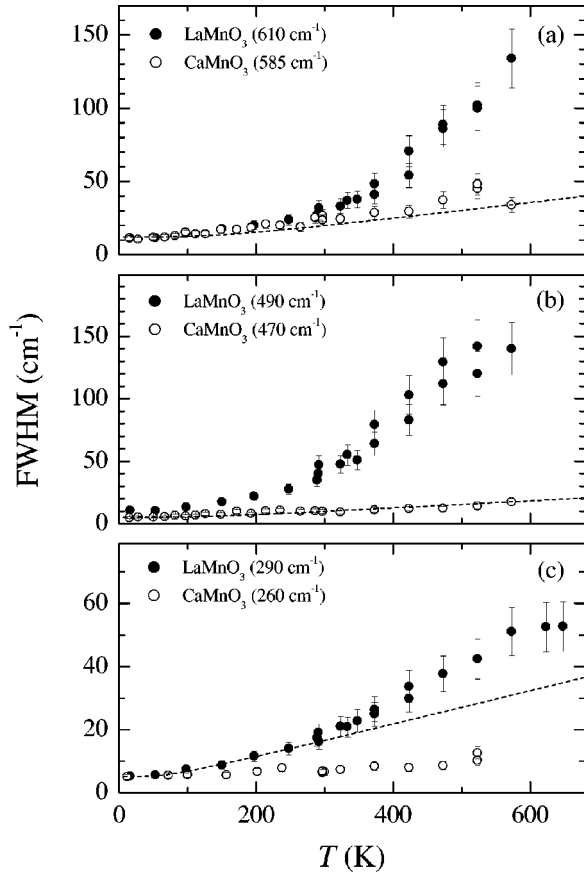


FIG. 3. T dependence of the linewidth for the stretching (a), bending (b), and rotational (c) modes of LaMnO_3 (closed circles) and CaMnO_3 (open circles). The lines are the expected behavior for CaMnO_3 according to a second-order cubic anharmonicity (see text).

the high-energy ~ 490 and ~ 610 cm^{-1} modes that involve internal vibrations of MnO_6 octahedra²² [see Figs. 3(a) and (b)].

In displacive phase transitions, large peak broadening may be observed in the following cases: (i) in the soft mode of the transition,²⁵ and (ii) in hard modes where the frequency change considerably through the transition (inhomogeneous broadening).²⁶ The ~ 490 and ~ 610 cm^{-1} peaks of LaMnO_3 are hard modes with a small frequency dependence on the JT distortion of the MnO_6 octahedra and on T [see Fig. 2(a)].^{13,27} Also, the linewidth of all the three studied modes remains finite above the T_{JT} [see Fig. 2(a)], indicating that none of them may be attributed to the transition.²⁵ Thus the dramatic broadening observed for these modes as T approaches T_{JT} from below is not consistent with a displacive JT phase transition. Therefore the broadening should be a consequence of an increasing lattice disorder as T approaches T_{JT} . We should mention that the rotational-like mode of LaMnO_3 , at 290 cm^{-1} at $T = 10$ K, softens to ~ 220 cm^{-1} at $T = 720$ K [see Fig. 2(a)], i.e., it is a soft mode, similarly to rhombohedral perovskites with D_{3d}^6 space group.²⁸ But, this vibration is not a JT mode²² and its frequency remains high at T_{JT} . Therefore this softening is not associated with the JT transition, and is possibly due to a reduction of the average tilt angle of the MnO_6 octahedra as T increases.⁹

The results discussed above strongly suggest that the JT transition of LaMnO_3 has an order-disorder character, confirming the prediction given by Millis¹⁷ and Zhou and Goodenough.¹⁵ Although the JT transition in LaMnO_3 is being associated to an order-disorder one, relevant differences are observed between the JT transition in LaMnO_3 and the order-disorder transitions found in other perovskite compounds. Particularly, the anomalous broadening of the hard modes is at least one order of magnitude bigger than those usually found in order-disorder phase transitions for other perovskites,¹⁸ and it is observed even at T well below T_{JT} (see Fig. 3). These results can be understood assuming the following scenario for the JT transition in LaMnO_3 . At $T = 10$ K, the oxygen octahedra show a cooperative JT distortion associated with the ordering of the Mn^{3+} e_g orbitals through the crystal lattice. The long phonons mean lifetime observed at this temperature (narrow lines), indicates low defect concentration, good crystallinity, and high ordering in our sample, consistent with local structure pair distribution function studies in a similar sample at low T .¹¹ As T increases, due to a thermally activated disorder of the orientation of the e_g orbitals in some of the Mn^{3+} ions, local deviations from the mean crystal structure and a consequent disorder in the oxygen network is expected. Such structural fluctuations may decrease the phonons mean lifetime and account for the anomalous phonon broadenings observed in LaMnO_3 . As T approaches T_{JT} , the structural fluctuations are large enough to break the cooperativeness of the orbital ordering, leading to an average ‘‘cubic’’ crystal structure at the JT transition.^{9,10} It is interesting to mention that the measured values of the phonon linewidths at $T = 520$ K for LaMnO_3 , in particular for the bending and stretching modes, are of the order of those found in amorphous materials, suggesting the existence of a high level of structural disorder well below the JT transition temperature. For $T > T_{JT}$ the average crystal structure is metrically cubic, with no cooperative JT distortion of the MnO_6 octahedra.⁹ However, according to the scenario suggested above, the crystal lattice is also disordered above the JT transition. In this high- T phase only short-range orbital ordering may still persist, or, alternatively, the orientation of the Mn^{3+} e_g orbitals may be completely disordered.

As mentioned earlier, the LaMnO_3 ceramic sample studied in this work shows a non-negligible proportion of Mn^{4+} ions ($\sim 2.5\%$). In general, the large reduction of T_{JT} observed in nonstoichiometric LaMnO_3 samples^{8,15} may be ascribed to an additional contribution to the orbital disorder caused by the absence of e_g orbitals in the Mn^{4+} ions. However, it is clear from the small phonon linewidths observed in our sample at low temperatures (see Figs. 2 and 3) that the thermal-activated disorder is still the determinant effect that leads to the Jahn-Teller transition at 705 K in this sample. Differently, for $\text{La}_{1-x}\text{Mn}_{1-x}\text{O}_3$ compounds showing a Mn^{4+} concentration $\geq 5\%$, the Raman-active phonons are considerably broad even at low T ,²⁷ indicating that the lattice disorder caused by cationic vacancies is playing an important role for such samples.

In summary, Raman-scattering measurements were performed in LaMnO_3 over a wide temperature range, including

the Jahn-Teller transition ($T_{JT} \sim 705$ K). A dramatic broadening was observed for all the Raman modes below T_{JT} . An order-disorder scenario, based on the thermal-activated disorder of the $\text{Mn}^{3+} e_g$ orbitals, was invoked to describe the high- T orthorhombic-to-cubic transition in LaMnO_3 .

This work was supported by CNPq Grant Nos. 910102/96-1 and 301338/77-9, FAPESP Grant Nos. 96/4625-8, 96/12585-6, 97/03065-1, 97/11563-1, 97/12648-0, 98/614-7, and 98/14521-0, Brazil, NSF-DMR Nos. 9705155 and NSF-INT 9602928, USA.

*Present address: NIST Center for Neutron Research, National Institute of Standards and Technology, Gaithersburg, MD 20899 and Center for Superconductivity Research, Department of Physics, University of Maryland, College Park, MD 20742.

¹R.M. Kusters *et al.*, *Physica B* **155**, 362 (1989); S. Jin *et al.*, *Science* **264**, 413 (1994); R. von Helmolt *et al.*, *Phys. Rev. Lett.* **71**, 2331 (1993).

²C. Zener, *Phys. Rev.* **82**, 403 (1951).

³A.J. Millis *et al.*, *Phys. Rev. Lett.* **74**, 5144 (1995).

⁴E.O. Wollan and W.C. Koehler, *Phys. Rev.* **100**, 545 (1955).

⁵J.B. Goodenough, *Phys. Rev.* **100**, 564 (1955); J. Goodenough *et al.*, *ibid.* **124**, 373 (1961).

⁶A. Wold and R. Arnott, *J. Phys. Chem. Solids* **9**, 176 (1959); J.B.A.A. Elemans *et al.*, *J. Solid State Chem.* **3**, 238 (1971); J. Töpfer and J.B. Goodenough, *ibid.* **130**, 117 (1997).

⁷A.K. Bogush *et al.*, *Cryst. Res. Technol.* **18**, 589 (1983).

⁸M. Tovar *et al.*, *Phys. Rev. B* **60**, 10 199 (1999); F. Prado *et al.*, *J. Magn. Magn. Mater.* **196-197**, 481 (1999).

⁹J. Rodríguez-Carvajal *et al.*, *Phys. Rev. B* **57**, R3189 (1998).

¹⁰P. Norby *et al.*, *J. Solid State Chem.* **119**, 191 (1995).

¹¹Th. Proffen *et al.*, *Phys. Rev. B* **60**, 9973 (1999).

¹²J.F. Mitchell *et al.*, *Phys. Rev. B* **54**, 6172 (1996); F. Moussa *et al.*, *ibid.* **54**, 15 149 (1996); Q. Huang *et al.*, *ibid.* **55**, 14 987 (1997); C. Ritter *et al.*, *ibid.* **56**, 8902 (1997).

¹³E. Granado *et al.*, *Phys. Rev. B* **60**, 11 879 (1999); **58**, 11 435 (1998); V.B. Podobedov *et al.*, *ibid.* **58**, 43 (1998).

¹⁴I. Solovyev *et al.*, *Phys. Rev. Lett.* **76**, 4825 (1996); S. Satpathy *et al.*, *ibid.* **76**, 960 (1996); H. Sawada *et al.*, *Phys. Rev. B* **56**, 12 154 (1997); L.F. Feiner and A.M. Oleś, *ibid.* **59**, 3295 (1999); J.W. Liu *et al.*, *ibid.* **60**, 12 968 (1999); T. Hotta *et al.*, *ibid.* **60**, R15 009 (1999).

¹⁵J.-S. Zhou and J.B. Goodenough, *Phys. Rev. B* **60**, R15 002 (1999).

¹⁶G.H. Jonker, *Physica (Amsterdam)* **22**, 707 (1956).

¹⁷A.J. Millis, *Phys. Rev. B* **53**, 8434 (1996).

¹⁸For a recent review, see E. Husson, *Key Eng. Mater.* **155-156**, 1 (1998).

¹⁹W. Cochran, *Adv. Phys.* **9**, 387 (1960); **10**, 401 (1961).

²⁰S.B. Oseroff *et al.*, *Phys. Rev. B* **53**, 6521 (1996).

²¹J.J. Neumeier and D.H. Goodwin, *J. Appl. Phys.* **85**, 5591 (1999).

²²M.N. Iliev *et al.*, *Phys. Rev. B* **57**, 2872 (1998).

²³P.G. Klemens, *Phys. Rev.* **148**, 845 (1966); M. Balkanski, R.F. Wallis, and E. Haro, *Phys. Rev. B* **28**, 1928 (1983).

²⁴E. Liarokapis *et al.*, *Phys. Rev. B* **60**, 12 758 (1999).

²⁵J.A. Sanjurjo *et al.*, *Phys. Rev. B* **28**, 7260 (1983).

²⁶S.A.T. Redfern, *Phys. Rev. B* **48**, 5761 (1993).

²⁷E. Granado *et al.*, *Phys. Status Solidi B* **220**, 609 (2000).

²⁸J.F. Scott, *Phys. Rev.* **183**, 823 (1969).